JOURNAL OF MATERIALS SCIENCE 30 (1995) 4884–4889

Optical and electrical properties of electrodeposited silver based thin films

P. RAVISELVAN, ABDUL KARIEM AROF*, S. RADHAKRISHNA
*Institute for Advanced Studies and * Physics Division, Centre for Foundation Studies in Science, Universiti Malaya, 59 100 Kuala Lumpur, Malaysia*

The electrodeposited superionic conductor $Ag_6I_4WO_4$ was doped with various concentrations of $[CrO_4]^{2-}$ to form the quarternary compound $Ag_6I_4WO_{4(1-x)}CrO_{4(x)}$. The doping level, x, was varied from 0 to 0.6 and the optimum compound was used for further analysis. X-ray diffraction (XRD) analysis indicated major peaks occurring at d values of 3.75, 2.29, 1.96 and 3.96 in the order of decreasing intensity. The energy dispersive analysis of X-rays (EDAX) technique verified quantitatively the ratio of the components in the solid electrolyte. From the fringes seen in the interference pattern of the transmission spectrum, the refractive index and thickness of the film was calculated. The absorption spectrum indicated the characteristic chromate peak at 310 nm when the dopant was present. An open circuit voltage (OCV) of 670 mV was observed for the fabricated cells with optimum performance at a doping level of $x = 0.1$, where the best discharge characteristics were observed. The subsequent conductivity was calculated to be of the order $10^{-3}\Omega^{-1}\,cm^{-1}$ from the Cole–Cole plot.

1. Introduction

The study to find ionic materials with high conductivity has uncovered numerous superionic conductors which have become the focus of interest in recent years [1, 2]. These materials are known to have properties that are feasible for practical uses, such as solid state batteries and electrochemical devices.

Silver based materials are fast ion conductors, but often they are not suitable to be commercially useful at room temperature. The conductivity of such materials is known to be enhanced if the material is doped with additional impurities [3–5]. The purpose of incorporating oxide dopants is to modify the lattice structure for the improved mobility of silver ions. Many superionic materials have been derived from silver for studies involving structural, transport and physical characteristics. The method of electrodeposition is a good way of preparing superionic conductors due to the ease of preparation and accuracy of deposition as shown in earlier work [6–8]. The other methods that have been employed in the preparation of $Ag_6I_4WO_4$ are aqueous deposition [9] and vacuum melting of its constituents [3].

In this work, the optical and electrical properties of the quarternary fast ion conducting compound $Ag_6I_4WO_{4(1-x)}CrO_{4(x)}$ are studied. This material has been synthesized by varying the dopant concentration $[CrO_4]^{2-}$ in the solid electrolyte $Ag_6I_4WO_4$. Previous studies have also shown that the Ag^+ mobile ions in silver tungstate ($Ag_6I_4WO_4$) electrolytes have a conductivity of the order $10^{-2}\,\Omega^{-1}\,cm^{-1}$ [10–12] and $Ag/Ag_6I_4WO_4/I_2$ cells have been known to give an open circuit voltage of 687 mV [4].

2. Experimental procedure

2.1. Sample preparation

The method of electrodeposition was employed for preparing the material. Two identical silver plates of 99.9% purity were used as electrodes. Earlier studies [9] outlined the ideal parameters of deposition and some of these have been followed closely to obtain good deposition conditions. Analar grade sodium tungstate (99%) and a 56% solution of hydroiodic acid were used as the starting materials for the preparation of the electrolyte. A solution of sodium tungstate and a dilution of the acid were added together with the molar ratio of 1:4. This electrolyte was used in the fabrication of $Ag_6I_4WO_4$.

The silver plates were held by an insulating separator and dipped in the electrolyte and a potential was applied across them from a regulated power supply. The current flow was monitored throughout the process. An initial study indicated that the optimum quality samples were obtained with an applied potential of 5 V and a plate separation of 4 cm. Through a process similar to electrolysis, the required deposition was obtained on the anode plate.

For the preparation of $Ag_6I_4WO_{4(1-x)}CrO_{4(x)}$, carefully calculated amounts of potassium chromate (K_2CrO_4) were introduced in the earlier electrolyte at various doping concentrations to maintain the ratio of $WO_{4(1-x)}CrO_{4(x)}$ and to ensure the molar ratio of this compound and hydroiodic acid (HI) was at 1:4. The deposition was then dried in an oven at 120 °C for 1 h.

0022–2461

2.2. Material Analysis

2.2.1. X-ray diffraction analysis

XRD was carried out using a Shimadzu X-ray diffractometer with CuK_α radiation ($\lambda = 0.15418$ nm) to deduce the phase of the material as well as for crystal identification and orientation. The effects of $[CrO_4]^{-2}$ doping on the diffractogram were subjects of interest. The samples for this analysis were prepared by smearing a small quantity of finely ground electrolyte onto a section of a microscope slide prior to mounting it into the sample compartment.

2.2.2. Quantitative analysis

Quantitative analysis of the material was carried out using energy dispersive analysis of X-rays technique on the EDAX system coupled with a Philips 515 scanning electron microscope (SEM). The materials were mounted on aluminium stubs with graphite glue for this purpose.

2.2.3. Optical analysis

Due to the opaque nature of the electrolyte formed on the electrodes, conventional methods of optical analysis were not possible. A small quantity of the sample was ground into a talcum texture. The sample was then dissolved in acetone and smeared evenly onto a thoroughly cleaned microscope slide and left to dry. These films of electrolytes were subsequently used in all the optical analyses. The Shimadzu UV-3101PC was used for ultra violet (u.v.) and visible analysis. In these analyses, both the absorption and transmission spectra were recorded. A diffractogram was also done on these types of samples to ensure that dissolving in acetone had no effect on the deposited material in terms of the phase and chemical composition.

2.3. Electrical properties

The electrodeposited superionic conductors were fabricated into cells in the form of pellets of 13 mm diameter and 0.5 mm thickness at a pelletizing pressure of 14 MPa. The configuration of the cells were Ag + electrolyte/electrolyte/ I_2 + carbon + electrolyte, which is known to have a better cell performance in comparison to Ag/Electrolyte/I_2 [13]. The mass of the cell composition is shown below

Anode	
Ag	0.10 g
Electrolyte	0.10 g
Electrolyte	0.50 g
Cathode	
I_2	0.10 g
Carbon	0.10 g
Electrolyte	0.02 g
Total mass	0.92 g

A Hioki (3520) bridge was used to measure the a.c. conductivity in the frequency range 1–100 KHz. The bulk resistance of the electrolyte, R_B, was obtained from the Cole–Cole plot for conductivity calculations.

The internal resistance of the cell was obtained following a method that has been described elsewhere [14]. The cells were then discharged at a constant current of 50 μA. From this curve, the discharge capacity and energy density of the cell were calculated.

3. Results and discussion

The superionic conductor $Ag_6I_4WO_{4(1-x)}CrO_{4(x)}$ was fabricated by varying the ratio x, from 0 to 0.6 in steps of 0.1. All depositions were done at 27 °C and at a current density of 2 mA cm^{-2}. The best cell properties were obtained at $x = 0.1$.

In the electrodeposition process, a reaction somewhat similar to electrolysis occurred where the anions and cations in the electrolyte moved to the anode and cathode, respectively. The following electrode reactions took place

At anode

$$Ag \rightarrow Ag^+ + e^- \text{ (oxidation)}$$

$$6Ag^+ + 4I^- + [WO_{4(1-x)}]^{-2} + [CrO_{4(x)}]^{-2} \rightarrow Ag_6I_4WO_{4(1-x)}CrO_{4(x)}$$

At cathode

$$H^+ + e^- \rightarrow H \text{ (reduction)}$$

$$H + H \rightarrow H_2 \text{ (gas)}$$

The solid electrolyte synthesized as an even yellow-green deposition on the anode. The following data presented will emphasize $Ag_6I_4WO_{4(0.9)}CrO_{4(0.1)}$, which apparently gives the best galvanic cell performance and $Ag_6I_4WO_4$ is used as a reference point for comparison. The deposited solid electrolyte was subjected to annealing at 100 °C for 1 h prior to analysis.

3.1. Characterization studies

The major peaks observed from the X-ray diffractogram are listed in Table I. The diffractogram for the material of concern is given in Fig. 1.

The sharpness of the bands in the diffractogram indicates the material deposited is not an amorphous medium but crystalline in nature. The superionic conductor, $Ag_6I_4WO_4$, deposited did not have any strong peaks corresponding to Ag_2WO_4, $Ag_5IW_2O_8$, $Ag_4I_2WO_4$ or AgI_n [12]. The close relationship of the peaks as reported for $Ag_6I_4WO_4$ [3] supports the identification of the deposition. The extra peaks noticed with increasing values of x could be attributed to the progressive amounts of CrO_4 used in the material synthesis. The additional lines could indicate a mixed phase that could be denoted by $AgI–Ag_yI_zWO_{4(1-x)}$-$CrO_{4(x)}$, where the AgI presence is quite obvious due to corresponding lines. Repeated analysis indicates that this compound is reproducible each time and does not decay within a time frame of one month.

When CrO_4 is introduced, a slight d value shift of the peaks, in the order of 10 picometer is observed. This could be attributed to the slightly increased interatomic spacing when an additional ion of the same

TABLE I X-ray diffraction results for $Ag_6I_4WO_4$ and $Ag_6I_4WO_{4(0.9)}CrO_{4(0.1)}$

Present data				Reported data		
$Ag_6I_4WO_4$		$Ag_6I_4WO_{4(0.9)}CrO_{4(0.1)}$		AgI		$Ag_6I_4WO_4$
d(nm)	I/I_0 (%)	d(nm)	I/I_0(%)	d(nm)	I/I_0 (%)	d(nm)
0.393	15	0.397	19	0.375	100	0.444
0.371	100	0.374	100	0.230	70	0.425
0.221	73	0.352	7	0.196	40	0.413
0.195	43	0.229	62			0.379
0.148	6	0.215	7			0.368
0.132	8	0.196	40			0.348
0.125	5	0.149	7			0.318
0.124	5	0.133	7			0.296
0.110	4	0.125	5			0.292
		0.124	5			0.287
						0.271
						0.256
						0.246
						0.238
						0.231
						0.218
						0.193

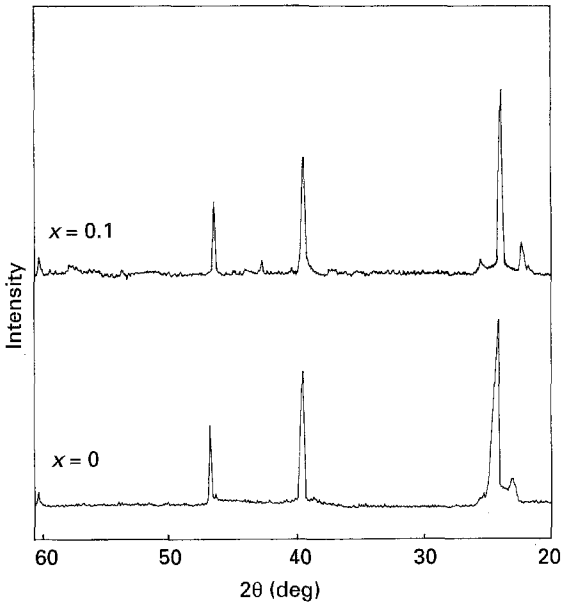

Figure 1 The X-ray diffractogram for $Ag_6I_4WO_{4(1-x)}CrO_{4(x)}$ at $x = 0$ and $x = 0.1$.

valence as tungstate is introduced into the solid electrolyte.

Quantitative characterization was used to verify further the nature of the deposited material. The EDAX data for $Ag_6I_4WO_4$ and $Ag_6I_4WO_{4(0.9)}$-$CrO_{4(0.1)}$, as compared with theoretical values are shown in Table II. The actual EDAX spectrum obtained is given in Fig. 2.

It is quite evident that the EDAX data show a close correlation between the relative and theoretical composition percentages. These data further support the identification of the sample deposited and clearly show the presence of chromium.

TABLE II Quantitative comparison between obtained and calculated data

	Element	Present (%)	Theoretical(%)
$Ag_6I_4WO_4$	Ag	54.48	48.36
	I	34.26	37.92
	W	10.26	13.72
$Ag_6I_4WO_{4(0.9)}CrO_{4(0.1)}$	Ag	51.07	48.84
	I	35.46	38.29
	W	12.93	12.48
	Cr	0.54	0.39

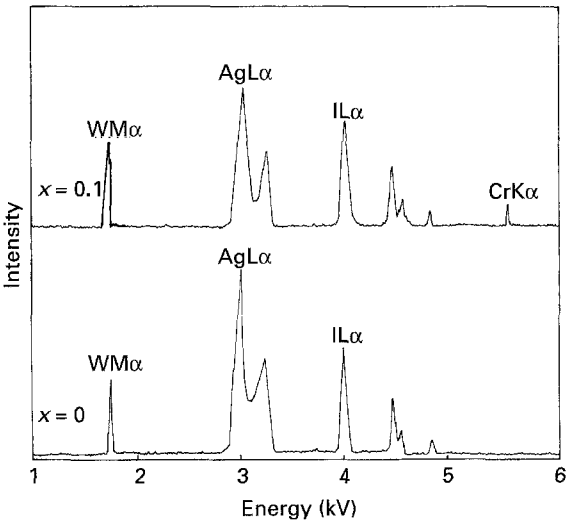

Figure 2 The EDAX spectrum for $Ag_6I_4WO_{4(1-x)}CrO_{4(x)}$ at $x = 0$ and $x = 0.1$.

3.2. Ultraviolet and visible (u.v./vis) optical characterization

In the transmission spectrum of the u.v./vis region, an interference fringe pattern was observed. This

occurrence of transmission fringes is due to the atomic transitions between discrete energy bands and helps deduce the refractive index of the film, the absorption coefficient and the thickness of the film coated on a glass substrate.

From the spectrum, the following data are extracted

1. λ_1 and λ_2 that are peaks of two selected fringes; and

2. $T_{\lambda 1}$ max, $T_{\lambda 1}$ min, $T_{\lambda 2}$ max, $T_{\lambda 2}$ min, which are the maximum and minimum transmission values at the minimum transmission values at the two selected wavelengths.

The refractive index of the superionic conductor is given by

$$n(\lambda) = [N + (N^2 - n_0^2 n_1^2)^{1/2}]^{1/2}$$

where

$$N = \frac{n_0^2 + n_1^2 + 2n_0 n_1}{2} \times \frac{T_{max} - T_{min}}{T_{max} \times T_{min}}$$

where n is explicitly determined from T_{max}, T_{min}, n_1 and n_o at a particular wavelength. n_1 and n_o are the refractive index of glass and air, respectively.

Knowing n, one can determine the absorption coefficient, α, from

$$\alpha = \frac{C_1[1 - (T_{max}/T_{min})^{1/2}]}{C_2[1 + (T_{max}/T_{min})^{1/2}]}$$

where $C_1 = (n + n_o)\ (n_1 + n)$ and $C_2 = (n - n_o)\ (n_1 - n)$

The film thickness, t, can be calculated from two of the fringes in the spectrum using the equation

$$t = \frac{M\lambda_1\lambda_2}{2[n(\lambda_1) \times \lambda_2 - n(\lambda_2) \times \lambda_1]}$$

where $\lambda_2 > \lambda_1$ and M is the number of oscillations between two extremes.

The information above is calculated and tabulated in Table III. Fig. 3 shows the transmission spectrum of the deposited material when $x = 0$ and $x = 0.1$.

From the data in Table III, it can be noted that the refractive index, n, decreases and the subsequent absorption coefficient, α, increases upon the presence of $[CrO_4]^{-2}$ in the deposited material. The absorption spectrum, as shown in Fig. 4, shows a strong band at 310 nm attributed to the discrete chromate anion when $x = 0.1$. This information is required as EDAX data could only show the chromium content and not chromate, qualitatively. As a basis of comparison, no peak at such wavelength region is noted at $x = 0$, where no chromate is used in the material fabrication.

TABLE III Comparison between the optical properties of deposited electrolyte

Properties	$Ag_6I_4WO_4$ ($x = 0$)	$Ag_6I_4WO_{4(0.9)}$-$CrO_{4(0.1)}$ ($x = 0.1$)
1. Refractive index	1.92	1.73
2. Absorption coefficient	0.28	0.57
3. Film thickness	0.18×10^{-6} m	0.71×10^{-6} m

Such a band has been reported earlier in chromate doped crystals [15].

3.3. Electrical characteristics

The first intersection on the x-axis of the Cole–Cole plot indicates bulk resistance, R_B, of the solid electrolyte. The ionic conductivity is calculated from the equation

$$\sigma = \frac{l}{R_B A}$$

where A and l are the surface area and thickness of the pellet, respectively.

The Cole–Cole plot for $x = 0$, 0.1 and 0.2 is shown in Fig. 5. Apparently the best galvanic cell properties were shown at the value $x = 0.1$, therefore a more thorough investigation was done by plotting the discharge characteristic curves in Fig. 6 and a voltage–current plot in Fig. 7. The discharge profile showed an initial drop in the voltage, which could have been due to the formation of a low conducting AgI layer at the cathode–electrolyte interface.

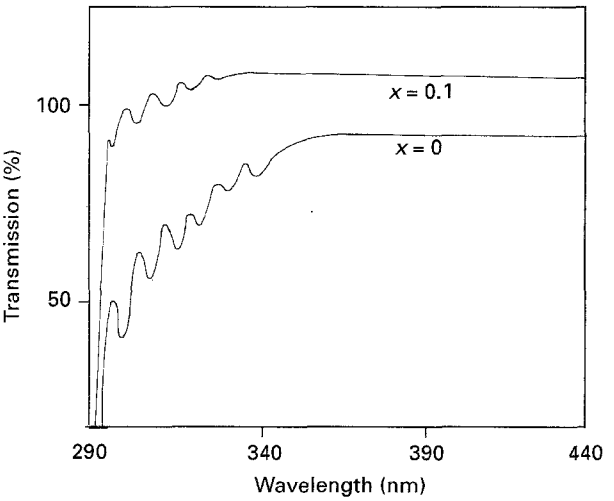

Figure 3 The transmission spectrum for $Ag_6I_4WO_{4(1-x)}CrO_{4(x)}$ at $x = 0$ and $x = 0.1$.

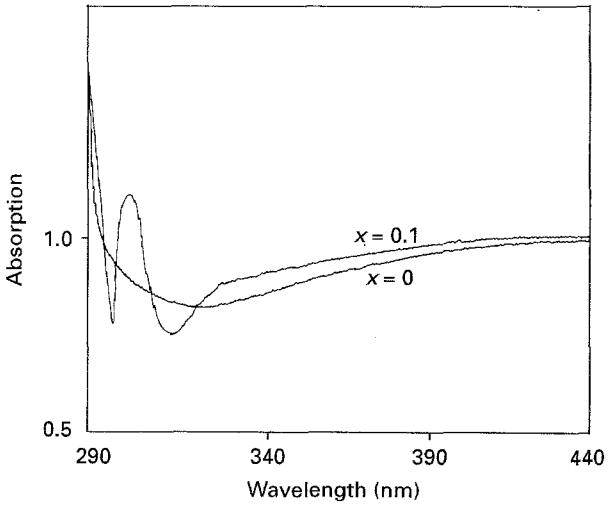

Figure 4 The absorption spectrum for $Ag_6I_4WO_{4(1-x)}CrO_{4(x)}$ at $x = 0$ and $x = 0.1$.

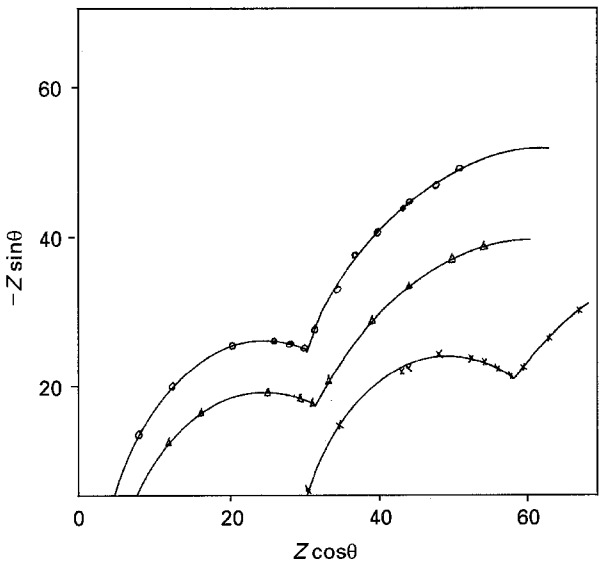

Figure 5 The Cole–Cole plot for $Ag_6I_4WO_{4(1-x)}CrO_{4(x)}$ at $x = 0$ (*), $x = 0.1$ (-O-) $x = 0.2$ (-Δ-) Z is the impedance value of the sample for a particular phase angle, θ at frequency f where 1 kHz $\leq f \leq$ 100 kHz.

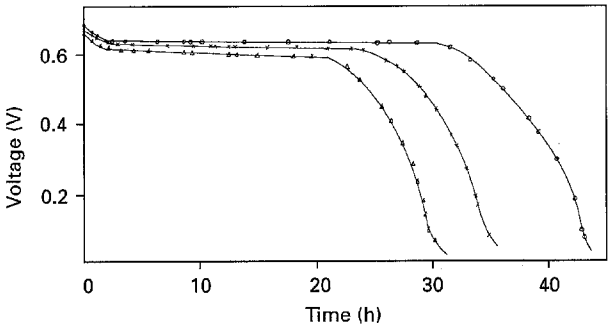

Figure 6 The discharge characteristic curve for $Ag_6I_4WO_{4(0.9)}$-$CrO_{4(0.1)}$ at $x = 0$ (*), $x = 0.1$. (-O-) and $x = 0.2$ (-Δ-).

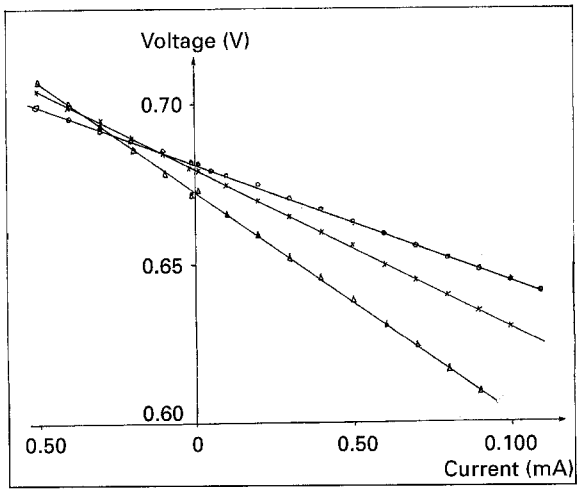

Figure 7 The I–V characteristic curve for $Ag_6I_4WO_{4(0.9)}CrO_{4(0.1)}$ at $x = 0$ (*), $x = 0.1$. (-O-) and $x = 0.2$ (-Δ-).

The cell then maintained an almost steady voltage (cutoff voltage) for a period of time (plateau time) before a sudden breakdown. Above a value of $x = 0.1$, a negative effect was shown in the galvanic cell properties, which could be due to chromate ions altering the lattice structure, adversely affecting the passage of silver ions.

TABLE IV Galvanic cell properties at $x = 0$, $x = 0.1$ and $x = 0.2$ (chromate concentration) for $Ag_6I_4WO_{4(1-x)}CrO_{4(x)}$

	$x = 0$	$x = 0.1$	$x = 0.2$
Conductivity, $\Omega^{-1}cm^{-1}$	1.25×10^{-3}	7.52×10^{-3}	4.70×10^{-3}
OCV, V (measured)	0.6820	0.6825	0.6771
Discharge time, h	35	43	30
Cutoff voltage, V	0.64	0.66	0.63
Current density, μAcm^{-2}	66.4	66.4	66.4
Discharge capacity, mA h^{-1}	1.3	1.6	1.1
Energy density W H^{-1} kg^{-1}	0.9043	1.1478	0.7533
Plateau time, h	26	32	22
Internal resistance, kΩ	5.016	3.515	6.717
OCV, V (calculated)	0.6810	0.6812	0.6721

From Fig. 6, the discharge capacity, D_c and the energy density were calculated from the equations below

$$D_c = I \times t_p$$

where I is the discharge current and t_p the plateau time. The energy density equals

$$\frac{V_p \times D_c}{w}$$

where V_p is the plateau voltage/cutoff voltage and w the weight of cell.

The conductivity and the open circuit voltage (OCV) together with various electrical characteristics measured and calculated are given in Table IV.

The internal resistance of the cells and the calculated OCV were obtained from the impedance-voltage (I–V) characteristic curve using the least square method, where the gradient represented the resistance and the intersection with the y-axis indicated the OCV.

4. Conclusion

It was conclusively found that the addition of chromate into $Ag_6I_4WO_4$ to form the quarternary compound $Ag_6I_4WO_{4(0.9)}CrO_{4(0.1)}$ improved the conductivity and increased the discharge time from 35 h for $Ag_6I_4WO_4$ to 43 h.

References

1. B. V. R. CHOWDARI and S. RADHAKRISHNA, "*Solid State Ionics Devices*" (World Scientific, Singapore, 1988) p. 726.
2. B. V. R. CHOWDARI, Q. LIU and L. CHEN, "*Recent Advances in Fast Ion Conducting Materials and Devices*" (World Scientific, Singapore, 1990) p. 601.
3. A. MAGISTRIS and G. CHIODELLI, *Electrochimica Acta* **26** (1981) 1241.
4. T. TAKAHASHI, S. IKEDA and O. YAMAMOTO, *J. Electrochem. Soc.* **119** (1972) 477.
5. S. A. SUTHANTHIRARAJ, A. M. SUKESHINI, K. HARIHARAN and P. MARUTHAMUTHU, *J. Mater. Sci. Lett.* **8** (1989) 965.
6. S. A. SUTHANTHIRARAJ and S. RADHAKRISHNA, *Cryst. Latt. Def. Amorph. Mater.* **11** (1985) 185.
7. *Idem. Solid State Ionics* **20** (1986) 45.

8. G. CHIODELLI, A. MAGISTRIS and A. SCHIRALDI, *Electrochimica Acta* **19** (1974) 655.
9. S. A. SUTHANTHIRAJ, PhD thesis, Indian Institute of Technology, Madras (1984).
10. A. MAGISTRIS, G. CHIODELLI and G. V. CAMPARI, *Z. Naturforsch.* **31a** (1976) 974.
11. S. A. SUTHANTHIRARAJ and B. BABUJI, *J. Electrochem.* **4** (1988) 389.
12. S. A. SUTHANTHIRARAJ, *Mater. For Solid State Batteries* (1986) 423.
13. R. V. G. K. SARMA and S. RADHAKRISHNA, *Solid State Ionics* **40/41** (1990) 483.
14. A. K. AROF, *J. Power Sources* **45** (1993) 255.
15. S. RADHAKRISHNA and K. P. PANDE, *Ion. Phys Stat. Solids* (*b*) **85** (1973) 155.

Received 4 August 1994
and accepted 22 March 1995